CHEMISTRY
A European Journal

A Journal of
ChemPubSoc Europe

Accepted Article

Title: Orthogonal ^{19}F-labeling for solid-state NMR reveals the conformation and orientation of short peptaibols in membranes

Authors: Stephan L. Grage, Sezgin Kara, Andrea Bordessa, Véronique Doan, Fabio Rizzolo, Marina Putzu, Tomáš Kubař, Anna Maria Papini, Grégory Chaume, Thierry Brigaud, Sergii Afonin, and Anne S. Ulrich

To be cited as: *Chem. Eur. J.* 10.1002/chem.201704307

Link to VoR: http://dx.doi.org/10.1002/chem.201704307

Supported by
ACES

WILEY-VCH

10.1002/chem.201704307

WILEY-VCH

FULL PAPER

Orthogonal ^{19}F-labeling for solid-state NMR reveals the conformation and orientation of short peptaibols in membranes

Stephan L. Grage,[a] Sezgin Kara,[b] Andrea Bordessa,[c] Véronique Doan,[c] Fabio Rizzolo,[c] Marina Putzu,[d] Tomáš Kubař,[d] Anna Maria Papini,[c] Grégory Chaume,[c] Thierry Brigaud,*[c] Sergii Afonin,*[a] Anne S. Ulrich*[a][b]

Abstract: Peptaibols are promising drug candidates in view of their interference with cellular membranes. Knowledge of their lipid interactions and membrane-bound structure is needed for understanding their activity and should be in principle accessible by solid-state NMR. However, their unusual amino acid composition and their non-canonical conformations make it very challenging to find suitable NMR labels. Especially in the case of short sequences, new strategies are required to maximize the structural information that can be obtained from each label. Here, we have combined trifluoromethylbicyclopentyl-*L*-glycine, (*R*)- and (*S*)-trifluoromethylalanine, and ^{15}N-backbone labels, each probing a different direction in the molecule, to elucidate the conformation and membrane alignment of harzianin HK-VI. For the short sequence of 11 amino acids we obtained 12 orientational constraints using ^{19}F- and ^{15}N-NMR. This strategy revealed a β-bend-ribbon structure, which becomes re-aligned in the membrane from a surface-parallel state towards a membrane-spanning state with increasing positive spontaneous curvature of the lipids.

Introduction

Fungi such as *Trichoderma* are producers of pharmaceutically attractive peptaibols that are endowed with improved biostability due to a high content of unconventional amino acids such as aminoisobutyric acid (Aib). The family of pept"Aib"ols can be grouped into long peptaibols (18-20 amino acids (aa), such as alamethicins), short peptaibols (11-16 aa, e.g. harzianins), and lipopeptaibols (7 or 11 aa, e.g. trichogins).[1] Many of these compounds exhibit cytotoxic activity, which is attributed to their ability to permeabilize membranes and form pores.[2,3,4,5,6] To decipher their mechanism of action, it is necessary to find out how the molecules are bound to a lipid bilayer, i.e. their conformation and their orientation relative to the membrane surface. Solid-state NMR analysis of oriented samples is an established method for obtaining such structural parameters in a quasi-native lipid environment, and selective ^{19}F-labels are the most sensitive and versatile NMR probes for membrane-active peptides.[7] An appropriate labeling strategy has to fulfill several requirements: (i) a sufficient number of labels to describe the alignment of any rigidly folded molecular segment with known conformation; (ii) these labels have to point into different directions such that orthogonal axes can be sampled; (iii) the labels have to be rigidly connected to the peptide backbone in order to translate their local orientations into the overall peptide alignment; and (iv) the labels have to be compatible with solid-phase peptide synthesis (SPPS). Long peptides (>20 aa) usually provide enough labeling sites, but opportunities for suitable conservative substitutions are very limited in short peptides/peptaibols.[7,8] It is important to avoid labels that point into similar directions, because this makes the orientational constraints partially redundant.[9,10] Another critical aspect in the case of peptaibols is their uncertain secondary structure, which requires extensive labeling to resolve the underlying backbone scaffold.

To address these challenges for the important class of short peptaibols, we report and validate a strategy that maximizes the amount of structural information that can be obtained from a small number of labelled sites. This approach is based on the use of complementary NMR reporter groups that provide non-redundant, "orthogonal" NMR structural constraints for one and the same position within a peptide sequence.

Here, we have combined four orthogonal NMR probes: (*R*)- and (*S*)-trifluoromethylalanine [(*R*)-CF_3-Ala, (*S*)-CF_3-Ala][8,11] are used to replace each Aib side chain one-by-one, while 3-(trifluoromethyl)-bicyclopent-[1.1.1]-1-yl-glycine (CF_3-Bpg)[12] in combination with ^{15}N-amide[13] in a suitable backbone position are used to replace single leucine or isoleucine residues (Figure 1A). This set of labels fulfils all criteria above: (i) it provides a chemical variety that allows conservative substitutions of many sites including Aib; (ii) the orthogonal labels (*S*)-CF_3-Ala, (*R*)-CF_3-Ala), CF_3-Bpg and amide-^{15}N sample four distinctly different director axes (Figure 1B); and (iii) they are rigidly connected to the peptide backbone. Regarding (iv), routine and efficient SPPS has been demonstrated for CF_3-Bpg incorporation.[12] However, the peptide coupling reactions were difficult in the case of the α-disubstituted

[a] Dr. S. L. Grage, Dr. S. Afonin, Prof. A. S. Ulrich
Institute of Biological Interfaces (IBG-2), Karlsruhe Institute of Technology (KIT), POB 3640, 76021 Karlsruhe (Germany)
E-mails: Sergiy.Afonin@kit.edu, Anne.Ulrich@kit.edu

[b] Dr. S. Kara, Prof. A. S. Ulrich
Institute of Organic Chemistry (IOC), KIT, Fritz-Haber Weg 6, 76131 Karlsruhe (Germany)

[c] Dr. A. Bordessa, V. Doan, Dr. F. Rizzolo, Prof. A. M. Papini, Dr. G. Chaume, Prof. T. Brigaud
Laboratoire de Chimie Biologique (LCB), EA4505, Plateform PeptLab@UCP, Université de Cergy-Pontoise, 5 Mail Gay-Lussac, Neuville sur Oise, 95000 Cergy-Pontoise cedex (France)
E-mail: Thierry.Brigaud@u-cergy.fr

[d] M. Putzu, Dr. T. Kubař
Institute of Physical Chemistry (IPC) & Center for Functional Nanostructures (CFN), KIT, 76131 Karlsruhe (Germany)

Supporting information and the ORCID identification number(s) for the author(s) of this article can be found under http://

10.1002/chem.201704307

CF_3-Ala isomers due to the low nucleophilicity of the nitrogen atom.[8,11,14] This problem has been bypassed by preparing in solution enantiomerically pure dipeptide building blocks, in which Leu or Ile is coupled to CF_3-Ala.[15] The dipeptides, including the ^{19}F-labeled Aib analogues could then be successfully introduced into peptaibols using microwave-assisted SPPS.

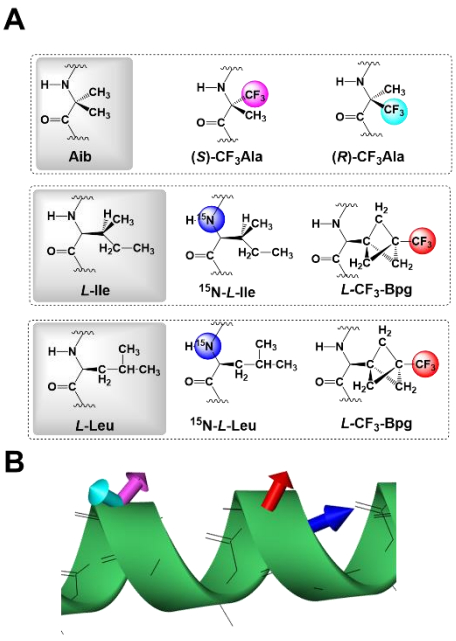

Figure 1. NMR labels used in this study. (A) Native amino acids (grey background) and used isostructural substitutions (with NMR reporter groups colored: ^{15}N – blue, ^{19}F – magenta in (*S*)-CF_3-Ala, cyan in (*R*)-CF_3-Ala, and red in CF_3-Bpg). (B) Sampled directions in space of the employed labels (colors as above) with respect to an ideal α-helical backbone.

As a representative short peptaibol, we selected here the natural 11mer harzianin HK-VI (HZ) with the sequence Ac-Aib-Asn-Ile-Ile-Aib-Pro-Leu-Leu-Aib-Pro-Leu-ol (Figure 2).[2,16] Even though the conformation and membrane alignment of the relatively long alamethicin has been extensively characterized, short peptaibols have been studied far less. A single experimental structure has been reported so far (on the 14mer harzianin HC-IX), revealing an unusual helical β-bend ribbon spiral fold in methanol.[1] The same non-extended conformation has been suggested for HZ,[16] but without resolving the actual backbone structure. To date, there is no structure available of any harzianin-type peptiabol in its functionally relevant membrane-bound state.

Results and Discussion

To introduce the selective ^{19}F-labels into HZ (Figure 2), we used microwave-assisted SPPS to synthesize four HZ analogues with CF_3-Bpg in one of the positions 3, 4, 7, and 8, and six analogues with (*R*)- or (*S*)-CF_3-Ala in positions 1, 5, and 9. For the latter ones, enantiomerically pure CF_3-Ala were prepared and linked to the preceding amino acid (Leu/Ile) to yield dipeptide building blocks suitable for automated Fmoc-synthesis, following specific protocols (see Supplementary Information, SI). In addition, four selectively ^{15}N-labeled HZ peptides were prepared with either ^{15}N-Leu or ^{15}N-Ile in one of the positions 3, 4, 7, and 8.

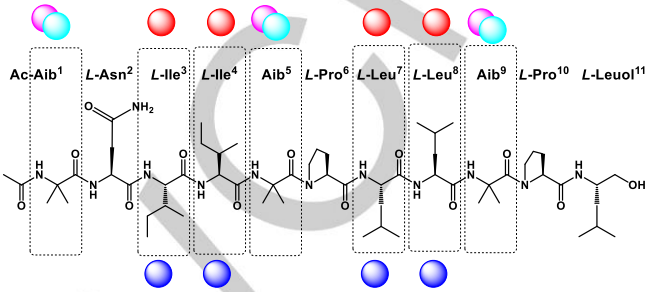

Figure 2. Amino acid sequence of harzianin HK-VI, illustrating the employed labelling scheme. Dashed boxes indicate the positions of the native amino acids, which were replaced by NMR labels, color symbols refer to the type of NMR label used in the marked positions: blue - ^{15}N, magenta - ^{19}F in (*S*)-CF_3-Ala, cyan - ^{19}F in (*R*)-CF_3-Ala, red - ^{19}F in *L*-CF_3-Bpg).

Before using the ^{19}F-labeled analogues for NMR analysis, we examined their conformation by circular dichroism (CD) in zwitterionic detergent micelles (Figure 3); similar results were obtained in other membrane-mimics, such as 50% 2,2,2-trifluoroethanol (TFE), micelles of sodium dodecyl sulfate (SDS), *n*-dodecylphosphocholine (DPC), lysoMPC (1-myristoyl-2-hydroxy-*sn*-glycero-3-phosphocholine), and in unilamellar vesicles composed of DMPC (1,2-dimyristoyl-*sn*-glycero-3-phosphocholine).

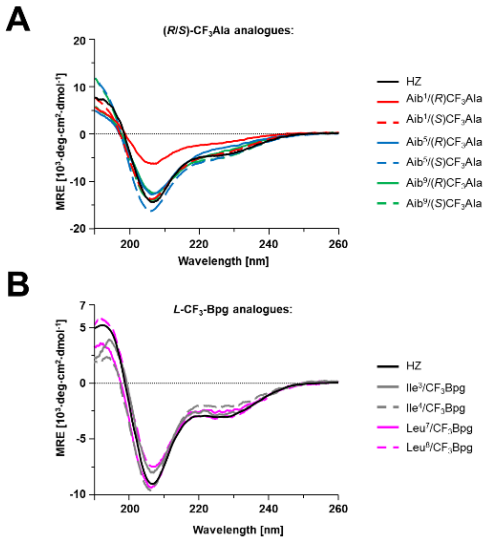

Figure 3. Representative CD spectra of selectively ^{19}F-labeled HZ analogues in membrane-mimicking environments. (A) Analogues with CF_3-Ala in the presence of lysoMPC micelles, and (B) analogues with CF_3-Bpg in the presence of DPC micelles. The peptides were mixed with preformed micelles in 10 mM phosphate buffer, pH 7.4, at a peptide/detergent molar ratio of 1/200.

All analogues gave the same CD lineshape as the wild type, hence the secondary structure remained unperturbed. Only the Ac-Aib[1] substituted analogue showed significant deviations presumably due to unfolding at the *N*-terminus. For this reason, position Aib[1] was excluded from further NMR analysis.

Notably, the CD spectra do not represent any common structural motif such as α-helix or β-strand, neither do they correspond to a random coil.[17] Also a dynamic transition between random coil/α-helix or a mixture thereof seems unlikely, given the similarity of the CD lineshapes in all the different environments. The peptide thus seems to adopt a unique and rather stable secondary structure. Similar CD spectra have been previously reported for peptaibols folded as 3_{10}-helices[18] and β-bend ribbon spirals.[19]

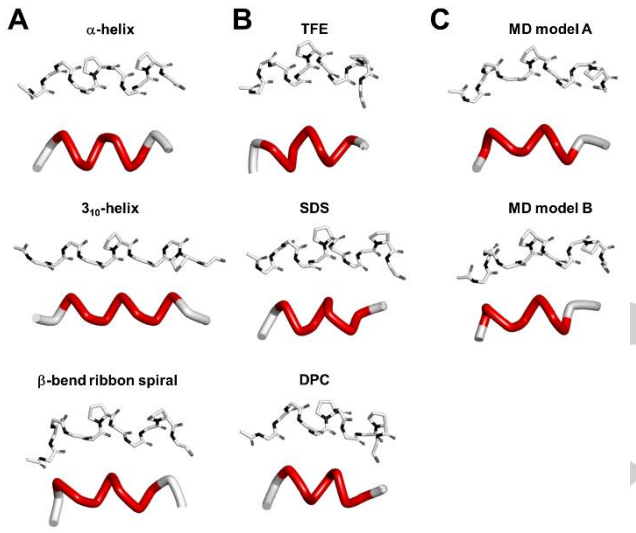

Figure 4. Structural models of HZ that were examined in the solid-state NMR data analysis. Backbone atoms and proline carbons are displayed in the stick representations (carbon – white, nitrogen – black, oxygen – light grey). The red stretch in the ribbons marks the fragment Ile^3-Aib^9 that was experimentally covered.

To analyze the membrane-bound peptaibol by solid-state NMR, is necessary to start off with a well-defined backbone structure. The orientation-dependent NMR data will then be iteratively evaluated in terms of both, the conformation and the alignment of the molecule within the membrane. Since CD did not provide a concrete secondary structure that could be used a model for the backbone, we generated a set of eight plausible structures (Figure 4) and tested whether they would be able to self-consistently predict the solid-state NMR data. As 3D models we considered: a continuous ideal α-helix (φ/ψ angles of -57°/-47°), a 3_{10}-helix (φ/ψ angles of -74°/-4°) and a β-bend ribbon spiral. The latter was generated as a homology model based on the liquid-state NMR structure of the 14mer harzianin HC-IX.[1] This peptaibol contains three similar Xxx-Yxx-Aib-Pro repeats (Xxx, Yxx = arbitrary amino acid), and the φ/ψ values averaged over all three repeats were used to model the corresponding "Ile-Ile-Aib-Pro" and "Leu-Leu-Aib-Pro" segments of HZ. In addition, we have resolved by liquid-state NMR the structure of HZ in 50% TFE, as well as in DPC and in SDS micelles.[20] Furthermore, two computational models were included, which we obtained as averaged structures from two independent unrestrained all-atom molecular dynamics (MD) simulations of HZ in a DMPC bilayer on a μs time scale.[21] (The backbone torsion angles φ/ψ of all models are listed in the SI Table S4).

Solid-state NMR structure analysis of membrane-bound peptides performed in macroscopically oriented samples and data analysis is based on the anisotropic ^{15}N chemical shift and the ^{19}F-^{19}F dipolar coupling within the CF_3-reporter group. The orientation-dependent ^{15}N chemical shifts δ_N are directly available from the signal position in the ^{15}N-NMR spectra of ^{15}N-labeled HZ (Figure 5A). The orientation-dependent intra-CF_3 dipolar couplings correspond to the triplet splittings Δ_{FF} in the ^{19}F-NMR spectra of the ^{19}F-labeled analogues (Figure 5B,5C). The orientation of the ^{15}N labeled moiety, given by two polar angles α and β relating the CSA principal axis frame to the membrane normal, can be deduced from:

$$\delta_N = \delta_{iso} + S_{mol}\,\delta_{CSA}\,(3\cos^2\beta - 1 + \eta\sin^2\beta\cos 2\alpha)/2, \qquad (\mathbf{1})$$

with the isotropic chemical shift δ_{iso} = 111 ppm, the asymmetry parameter η = -0.245, and the chemical shift anisotropy δ_{CSA} = 98 ppm. Similarly, the orientation of the CF_3-axis with respect to the membrane normal is related to the splitting by:

$$\Delta_{FF} = S_{mol}\,\Delta_0\,(3\cos^2\theta - 1)/2, \qquad (\mathbf{2})$$

with the maximum splitting Δ_0 = 16 kHz. Partial averaging of the anisotropies by motion of the peptide was taken into account by scaling the anisotropic contributions by an order parameter S_{mol}. For the analysis of the peptide orientation, the value of the ^{15}N chemical shift δ_N or the splitting Δ_{FF} was predicted for each label within a certain group of labels (using all labels or subsets thereof). For this, any given backbone model (or segment thereof) is placed into the membrane coordinate system in an orientation that is described by two angles τ and ρ (see SI Figure S2 for a graphical definition). Motional averaging is taken into account by scaling and the order parameter S_{mol}. To identify the best-fit orientation (i.e. particular combination of τ, ρ and S_{mol}), we numerically screened all possible combinations of τ, ρ and S_{mol} values and calculated δ_N or Δ_{FF} for all considered labels. The difference between the calculated and experimental NMR parameters was quantified by a root of mean square deviation (rmsd).

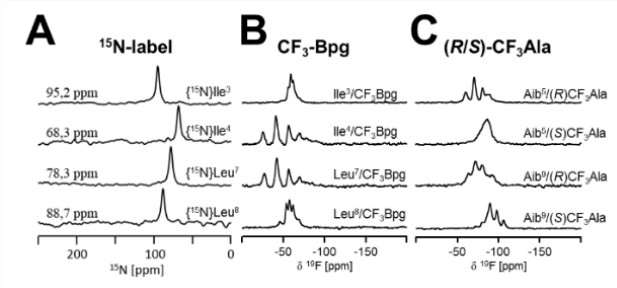

Figure 5. Solid-state ^{15}N- and ^{19}F-NMR spectra of HZ in oriented 1,2-diphytanoyl-*sn*-glycero-3-phosphocholine (DPhPC) bilayers, at 35°C.

10.1002/chem.201704307

The first, most straightforward attempt of using all eight ^{19}F labels at the same time in the data analysis resulted in a massive deviation of the predicted NMR parameters from the experimental data. This was the case for all of the 8 different structural models, giving errors well beyond the acceptable margins (see below). Therefore we decided not to use all NMR data simultaneously in the analysis, but only a subset of the labels representing one type of isotope label or a certain region within the sequence of HZ. We performed such data analyses several times, each time using a different selection of labels that we refer to as label "patterns". In particular, we analyzed the two peptide segments on either side of Pro^6 separately, while the other patterns covered the full length of HZ. Each pattern thus contained four orientational constraints, which is the mathematically required number of independent parameters to fully determine 3 structural variables (τ, ρ, and S_{mol}). These patterns include: all four ^{15}N-labels in positions 3, 4, 7, and 8 (pattern N3478); all four CF_3-Bpg labels in positions 3, 4, 7, and 8 (pattern F3478); all four (*R*)- and (*S*)-CF_3-Ala labels in positions 5 and 9 (pattern F59); the CF_3-Bpg and CF_3-Ala of the *N*-terminal half in positions 3, 4, and 5 (pattern F345); as well as the corresponding CF_3-Bpg and CF_3-Ala in the *C*-terminal half in positions 7, 8, and 9 (pattern F789).

In this way, we first validated the backbone structure and subsequently investigated more thoroughly the orientation of HZ in the lipid bilayer. When fitting the 8 different structural models, we obtain a best-fit value for each, though with different rmsd quality (see Table 1). Based on these numbers it is now possible to identify certain backbone models that match the experimental NMR data well, and to rule out others. If we accept all rmsd values below the experimental error as plausible, only few structures remain in agreement with the experiments.

Table 1. Quality of the best-fits to the NMR data, used to assess different structural models (see Figure 4) for HZ bound to DPhPC bilayers. The patterns of labels used in each analysis are indicated at the top. Experimental errors are 5 ppm and 1 kHz for the ^{15}N chemical shifts and ^{19}F-^{19}F dipolar couplings, respectively. The rmsd values within these margins are shown in bold.

	N3478	F3478	F59	F345	F789
	rmsd/ppm		rmsd/kHz		
α-helix	**4.68**	**0.44**	**0.51**	2.79	1.98
3_{10}-helix	**2.38**	2.46	1.75	3.21	2.27
β-bend ribbon	**1.15**	**0.40**	**0.26**	**0.52**	**0.66**
NMR(DPC)	**2.20**	**0.30**	**0.44**	1.65	1.46
NMR(SDS)	**2.75**	1.80	**0.14**	2.46	1.50
NMR(TFE)	**2.79**	2.79	**0.56**	1.70	1.70
MD model A	**2.63**	3.08	2.00	1.30	2.34
MD model B	6.20	2.97	2.00	**0.15**	2.04

On their own, the ^{15}N-NMR data are not conclusive in deciding the backbone structure, as most rmsd values are below or near the threshold given by the experimental error of ~5 ppm (pattern N3478). Likewise, the analysis of all CF_3-Ala labels (pattern F59) is not conclusive, as only the 3_{10}-helix and MD models can be ruled out as inconsistent candidates. Combining all CF_3-Bpg labels (pattern F3478), on the other hand, allows us to reduce the set of compatible models to α-helix, β-bend ribbon spiral, and the conformation in DPC micelles. The set of models can be narrowed down further using the two groups of ^{19}F-labels representing the *N*- and *C*-terminal segments of HZ. Considering the rmsd values of pattern F345 and F789, both of them clearly favor the β-bend ribbon spiral as the only model matching the solid-state NMR data (Table 1). This structure also produces very low rmsd for the other patterns (N3478, F3478, and F59), hence the β-bend ribbon spiral can be identified as the most likely backbone structure of HZ in DPhPC membranes. The same conclusion is reached when examining the combined set of data for HZ reconstituted in other lipids (see below, and SI Tables S6-S8). We can clearly rule out the 3_{10}-helix, which had earlier been discussed for Aib-rich structures and would have been compatible with the CD analysis.[18,22] Based on these results, we can now address and interpret the alignment of HZ in different lipid bilayers, by focusing on the orientation of the β-bend ribbon spiral that is given by the corresponding τ, ρ and S_{mol} values.

Two physical properties of membranes, namely the spontaneous lipid curvature and the bilayer thickness, are known to have a profound influence on peptide orientation.[23,24,25,26,27] We thus selected a series of phosphocholine systems allowing to examine both, decreasing thickness and increasing curvature (Figure 6): DPhPC, DMPC, 1,2-didecanoyl-*sn*-glycero-3-phosphocholine (DDPC), and a DMPC/lysoMPC mixture (molar ratio 2/1).

To evaluate and compare the orientation of HZ in these different lipid environments, additional NMR data was collected of all labeled analogues in oriented bilayers of the named lipid selection (see SI Figures S3-S6 for the spectra). These data were analyzed in terms of the HZ alignment, i.e. as the best-fit values τ, ρ, S_{mol} for the β-bend ribbon spiral. Again, these analyses were performed several times, each time including a different label pattern of ^{19}F-labels (patterns F3478, F59, F345 and F789) or ^{15}N-labels (N3478). The τ, ρ, S_{mol} values resulting from the individual label patterns were averaged and are summarized in Table 2.

Table 2. Membrane alignment of HZ in its β-bend ribbon spiral conformation (averages over the best-fit results of all patterns, see SI Tables S9-S12 for the non-averaged values), in oriented bilayers of lipids with different spontaneous curvature and thickness.

	DPhPC	DMPC	DDPC	DMPC/lysoMPC
τ	91°±29°	77°±12°	103°±30°	151°±17°
ρ	208°±15°	216°±14°	222°±17°	285°±26°
S_{mol}	0.66±0.10	0.68±0.21	0.38±0.15	0.34±0.12

The compact and rather hydrophobic peptaibol HZ has τ values of around 80°-90° (relative to the membrane normal) in DPhPC and DMPC, corresponding to an orientation of its long molecular axis parallel to the plane of the membrane. Such alignment is typically found for distinctly amphipathic molecules, such as cationic α-helical antimicrobial peptides.[23] Hydrophobic helices, on the other hand, typically adopt a transmembrane orientation.[27,28]. Interestingly, we find that with decreasing membrane thickness and increasing positive spontaneous

curvature, the tilt angle of HZ decreases to 100° in DDPC and to 150° in DMPC/lysoMPC, getting closer to an upright transmembrane orientation (Table 2, Figure 6). The peptide dynamics, too, reveal a clear change with the bilayer properties. High order parameter values of around ~0.7 are observed in DPhPC and DMPC, comparable to values typically found for α-helical surface-bound peptides.[29] These values decrease for HZ to ~0.4 in thin DDPC and DMPC/lysoMPC, where the peptide becomes even more mobile. The re-alignment of harzianin in highly curved DMPC/lysoMPC bilayers compares well with similar findings on amphiphilic antimicrobial peptides. In lipids with a highly positive spontaneous curvature they can flip into a transmembrane state and assemble as a stable pore.[25,26] In the case of HZ, both, surface-parallel and perpendicular alignments have been recently reported from MD simulations in DMPC, where a deep penetration of this hydrophobic molecule towards the core of the bilayer was observed.[21]

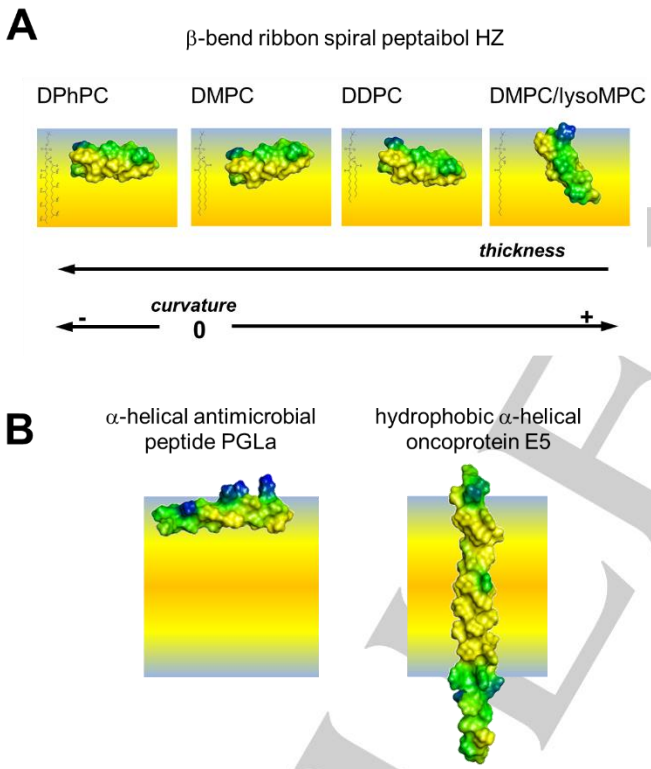

Figure 6. Orientation of HZ in bilayers of lipids with different spontaneous curvature and thickness as determined in this study (A). The polarity of HZ lies between the more polar typical antimicrobial peptides such as PGLa and hydrophobic transmembrane sequences such as the oncoprotein E5.[28,30] (B). Color encodes increasing polarity from yellow (hydrophobic) – green (intermediate) – blue (polar).

The observed re-alignment of HZ in bilayers with different lengths and spontaneous curvatures can provide new mechanistic insights into the membrane-perturbing activity of HZ. Compared to many well-known antimicrobial peptides, harzianin is quite short and more hydrophobic, besides being a peptaibol with an unusual conformation. Here, we observed an orientation of HZ parallel to the bilayer surface in the majority of lipid systems investigated, and MD simulations imply that the depth of insertion is deeper than for the typical amphiphilic α-helices. This alignment nonetheless agrees with the carpet mechanism that is considered to be one of several modes of action of membranolytic peptides: the binding and accumulation of peptides - when embedded near the polar/apolar interface - causes membrane thinning and/or micellization.[31] However, we also observed a considerable preference of HZ to tilt upright into the membrane in the presence of lipids with positive curvature or reduced thickness. Hence, the propensity of HZ to act via the conventional carpet mechanism may be questioned, because the surface activity of the peptide becomes reduced in the inserted state. Whether this ability to insert into the membrane is sufficient for HZ to assemble into oligomeric pores similar to those suggested for longer amphipathic peptides (or for the long peptiaibol alamethicin) should be debated in the light of its rather small size and its observed higher mobility in the inserted state. Given the much higher hydrophobicity of HZ as compared to typical cationic amphipathic antimicrobial peptides, in conjunction with its small size, the deeper penetration of HZ may be more effective and by itself sufficient to destabilize the lipid bilayer. The balance between a surface-parallel and an inserted alignment could also indicate a high ability of HZ to cross the lipid bilayer, allowing it to reach potential other targets inside the cell, different from the cellular membrane.

Conclusions

We have demonstrated and validated a general solid-state NMR approach, suitable to determine the structure and orientation of membrane-bound peptides. It is particularly relevant for sequences that offer only few positions for labeling, due to either a short length or an unusual amino acid composition and/or conformation. We used four orthogonal ^{19}F- and ^{15}N-NMR labels to sample different spatial orientations, which allowed us to collect several complementary NMR constraints even from a single labeled position in the peptide sequence. This way, the backbone structure and different alignment states of the peptaibol harzianin HZ VI could be determined, overcoming the special challenges imposed by the short sequence and high content of Aib of this peptide. Despite its hydrophobic character and its short length, harzianin HK-VI exhibits an alignment behavior that is also observed for longer and distinctly amphipathic sequences, such as α-helical antimicrobial and pore-forming peptides.[21] In membranes with negative or low spontaneous curvature harzianin HK-VI is preferentially aligned parallel to the bilayer surface, and it becomes tilted in lipids with high positive curvature. The short non-lipidated peptaibol may thus exhibit a lower membrane-perturbing activity via a carpet mechanism, as described for many membrane-perturbing peptides, but it may rather act by penetrating more deeply into the bilayer, and possess an enhanced ability to cross the membrane.

10.1002/chem.201704307

Experimental Section

Peptide synthesis. The synthesis of (*R*)/(*S*)-α-trifluoromethylalanine containing dipeptide building blocks for incorporation in HZ sequences was performed starting from unprotected enantiopure (*R*)- and (*S*)-CF_3-alanines which were synthesised according to our previously reported procedure involving a Strecker-type reaction on (*R*)-phenylglycinol derived trifluoromethyloxazolidines.[14] The following variations in synthetic procedures for the assembly of the dipeptides and characterisation of the compounds are detailed in the SI.

Unlabeled HZ was synthesized on a 0.25 mmol scale, using a SyroWave Biotage automated peptide synthesizer starting from H-*L*-Leucinol-2-chlorotrityl resin (loading: 0.5 mmol/g, 500 mg). Fmoc-Asn was coupled without any protecting group on the side chain. A double coupling was performed for each amino acid. Coupling reactions were accomplished with 3.0 equiv. of amino acid, 3.0 equiv. of HATU in DMF, and 4.2 equiv. of DIPEA in NMP, for 10 min at 70 °C, except for the Aib couplings, which were performed in two steps. The first step was performed at 55 °C for 15 min, and the second one was performed at 60 °C for 15 min. All Fmoc deprotections were carried out using 20% piperidine in DMF for 3 min and 12 min at room temperature. *N*-terminal acetylation of the peptide resin was performed by a repeated treatment with acetic anhydride (2.5 mmol) and NMM (2.5 mmol) in DCM for 1 h at room temperature. The 1,2-aminoalcohol peptide was cleaved from the resin upon four treatments with 30% HFIP in DCM for 30 min. The filtrates were combined and evaporated to dryness providing the crude peptide. The product was precipitated by addition of cold diethyl ether and then lyophilized. The crude peptide was purified by semi-preparative HPLC, using a Phenomenex Jupiter C18 (10 x 250 mm, 10 µm, flow: 4 mL/min) column, to yield the harzianin HK-VI (35 mg, 12 %, purity > 98%). The gradient elution system was composed of solvent A (0.1 % acetic acid in H_2O) and solvent B (0.1 % acetic acid in CH_3CN). Characterization of the products was performed by UPLC/MS on a Waters Acquity instrument coupled to a Waters 3100 detector with an analytical Waters BEH C18 column (2.1 x 50 mm, 1.7 µm, flow: 0.6 mL/min), and by HPLC using an Agilent Technologies 1200 series instrument with a ZORBAX Eclipse XDB-C18 analytical (4.6 x 150 mm, 5 µm) column operating at 1 mL/min or a Kinetex C18 (3 x 100 mm, 2.6 µm) column operating at 0.8 mL/min. For UPLC/MS and analytical HPLC the eluent system was composed of solvent A (0.1 % TFA in H_2O) and solvent B (0.1 % TFA in CH_3CN). Calcd. mass for $C_{58}H_{102}N_{12}O_{13}$ $[m+H]^+$: 1175.78, obs. mass (m/z): 1176.01.

Aib/CF_3-alanine substituted HZ analogues were synthesized and purified the same way, except that upon incorporation of the fluorinated dipeptide building blocks, a single coupling step (20 min at 60 °C) was performed. Calcd. mass for (Aib[1]/(*R*)CF_3Ala) $[m+H]^+$: 1229.75, obs. mass (m/z): 1229.85; Calcd. mass for $C_{58}H_{99}F_3N_{12}O_{13}$ (Aib[1]/(*S*)CF_3Ala) $[m+H]^+$: 1229.75, obs. mass (m/z): 1229.97; Calcd. mass for $C_{58}H_{99}F_3N_{12}O_{13}$ (Aib[5]/(*R*)CF_3Ala) $[m+H]^+$: 1229.75, obs. mass (m/z): 1230.36; Calcd. mass for $C_{58}H_{99}F_3N_{12}O_{13}$ (Aib[5]/(*S*)CF_3Ala) $[m+H]+$: 1229.75, obs. mass (m/z): 1230.30; Calcd. mass for $C_{58}H_{99}F_3N_{12}O_{13}$ (Aib[9]/(*R*)CF_3Ala) $[m+H]^+$: 1229.75, obs. mass (m/z): 1229.90; Calcd. mass for $C_{58}H_{99}F_3N_{12}O_{13}$ (Aib[9]/(*S*)CF_3Ala) $[m+H]^+$: 1229.75, obs. mass (m/z): 1229.96.

Lxx/CF_3-Bpg substituted HZ analogues were synthesized and purified the same way. Fmoc-CF_3-(*L*)-Bpg-OH was treated as Fmoc-Aib-OH. The syntheses were performed on a 0.15 mmol scale (resin loading: 0.5 mmol/g, 300 mg) and final cleavages succeeded upon a double treatment with TFA/DCM/water/TIS (47:47:4:2) for 1 h. Crude peptides were obtained from air flow-dried combined cleavage filtrates, which were lyophilized after addition of 5 mL of water. Calcd. mass for $C_{60}H_{99}F_3N_{12}O_{13}$ (Ile[3]/CF_3-Bpg) $[m+H]^+$: 1253.75, obs. mass (m/z): 1253.78; Calcd. mass for $C_{60}H_{99}F_3N_{12}O_{13}$ (Ile[4]/CF_3-Bpg) $[m+H]^+$: 1253.65, obs. mass (m/z): 1253.68; Calcd. mass for $C_{60}H_{99}F_3N_{12}O_{13}$ (Leu[7]/CF_3-Bpg) $[m+H]^+$: 1253.75, obs. mass (m/z): 1253.68; Calcd. mass for $C_{60}H_{99}F_3N_{12}O_{13}$ (Leu[8]/CF_3-Bpg) $[m+H]^+$: 1253.75, obs. mass (m/z): 1253.70.

The ^{15}N-Leu-containing HZ analogues were synthesised following the same procedure as for unlabeled HZ, except that they were synthesised on the 0.15 mmol scale. Calcd. mass for $C_{58}H_{102}N_{11}{}^{15}N_1O_{13}$ ({^{15}N}Leu[7]) $[m+H]^+$: 1176.77, obs. mass (m/z): 1176.68; Calcd. mass for $C_{58}H_{102}N_{11}{}^{15}N_1O_{13}$ ({^{15}N}Leu[8]) $[m+H]^+$: 1176.77, obs. mass (m/z): 1176.64.

The ^{15}N-Ile-containing HZ variants were synthesized using a Liberty Blue CEM automated peptide synthesizer, starting from H-*L*-Leucinol-2-chlorotrityl resin (loading: 0.5 mmol/g, 500 mg (^{15}N-Ile at position 3) or 280 mg (^{15}N-Ile at position 4)). A double coupling was performed for each amino acid. Coupling reactions were accomplished with 2.0 equiv. of ^{15}N-Fmoc-Ile-OH in DMF (0.1 M), 4.0 equiv. of amino acid in DMF (0.2 M), 4.0 equiv. of Oxyma pure in DMF (1.0 M), and 4.0 equiv. of DIC in DMF (0.5 M), for 2 min at 90 °C, except for the Fmoc-Aib-OH (at 50 °C for 10 min). Fmoc deprotections were carried out using 20% piperidine in DMF for 3 min at 75 °C, except for the Fmoc-Aib-OH (2x 10 min at 25 °C). The remainder of the synthesis followed the protocols used for unlabeled HZ. Calcd. mass for $C_{58}H_{102}N_{11}{}^{15}N_1O_{13}$ ({^{15}N}Ile[3]) $[m+H]^+$: 1176.77, obs. mass (m/z): 1177.14; Calcd. mass for $C_{58}H_{102}N_{11}{}^{15}N_1O_{13}$ ({^{15}N}Ile[4]) $[m+H]^+$: 1176.77, obs. mass (m/z): 1177.21.

The yields, purities, chromatography and mass spectroscopy data of the synthesized peptides are shown in SI.

Circular dichroism spectroscopy. The peptides were prepared as 1 mg/mL stock solutions in MeOH. Aliquots containing 0.1 mg peptide were transferred to 2 mL microcentrifuge tubes (LoBind Eppendorf), from which the solvent was removed by a flow of N_2, followed by incubation under vacuum overnight. The samples were briefly placed into a bath-sonicator and subsequently vortexed with 1 mL of the appropriate medium, consisting of either pure water (milli-Q ultrapure water), PB (10 mM phosphate buffer, pH 7.4), TFE/PB mixtures (TFE vol%: 40, 50, 75, 100), a solution of sodium dodecyl sulfate in milli-Q, a solution of *n*-dodecylphosphocholine in milli-Q, a solution of 1-myristoyl-2-hydroxy-*sn*-glycero-3-phosphocholine (lysoMPC) in milli-Q. The solutions with SDS, DPC and lysoMPC gave a peptide/detergent ratio of 1/200 mol/mol. Alternatively, the peptides were co-solubilized with DMPC in excess MeOH to achieve solutions with peptide/lipid ratios of 1/10, 1/20, 1/100 or 1/200 mol/mol. The organic solvent was removed by a flow of N_2, followed by incubation under vacuum overnight. The dry mixtures were resuspended in PB by a brief treatment in an ultrasonic bath and vortexing. Suspensions underwent 5-7 consecutive freeze/thaw/ultrasonication cycles to achieve large unilamellar vesicles with homogeneously reconstituted peptide.

The peptide/detergent/lipid mixtures were transferred into Hellma Suprasil quartz cuvettes with 1 mm path length. CD measurements were performed on a JASCO J-815 spectropolarimeter. Measurements were performed at 25 °C (solutions), or at variable temperatures (lipid suspensions). Spectra were acquired between 185 and 260 nm at 0.1 nm intervals (10 nm/min rate; 8 s response time; 1 nm bandwidth). Three consecutive scans were averaged for each sample and for the peptide-free samples (baseline). Baseline spectra were subtracted, the intensities at 260 nm were assigned to zero, and no smoothening was applied. All spectral processing was done using the Jasco Spectra Analysis software.

Solid-State NMR sample preparation. For solid-state NMR, labeled harzianin HK-VI was reconstituted into fully hydrated, mechanically oriented lipid bilayers on glass supports. First, ~0.25 mg of ^{19}F-labeled harzianin HK-Vi analogues or ~0.5 mg of ^{15}N-labeled harzianin HK-VI

analogues were co-dissolved in methanol or methanol/chloroform together with ~15 mg or 30 mg of lipid, respectively, to achieve a peptide/lipid ratio of 1/100 mol/mol. The solution was spotted onto about 20 glass slides (7.5 mm x 18 mm x 0.06 mm, Marienfeld, Germany), and the resulting films were dried under vacuum. The glass slides were then stacked and hydrated by incubation in 97% relative humidity at 48 °C overnight, which leads to the spontaneous formation of ~10^3 uniformly aligned and hydrated bilayers. The sample was wrapped in parafilm and a cling foil to prevent drying. The orientation of the sample was confirmed using solid-state ^{31}P-NMR. In all spectra shown here, the membrane normal was aligned parallel to the static magnetic field direction.

Solid-state NMR spectroscopy. Solid-state ^{19}F-NMR spectra were measured on a Bruker Avance III spectrometer with an 11.7 T widebore magnet, operating at a ^{19}F-resonance frequency of 470 MHz. The sample was placed into an in-house built ^{19}F/^{1}H double-resonance probe, equipped with a flat coil (rectangular cross section, 3 x 9 mm). NMR-spectra were acquired using an anti-ringing sequence to suppress any probe background signal, using a 90°-pulse length of 2.5 µs and 20 kHz ^{1}H decoupling.[32] Typically 2000 scans of 4 ms separated by a recycle delay of 2 s were collected.

Solid-state ^{15}N-NMR spectra of the oriented samples were measured on a Bruker Avance spectrometer with a 14.1 T widebore magnet, operating at a ^{15}N-resonance frequency of 60 MHz. The sample was placed into an in-house built ^{15}N/^{1}H double-resonance lowE probe, equipped with a flat coil (rectangular cross section, 3 x 9 mm). NMR-spectra were acquired following cross-polarization from ^{1}H (using radio-frequency amplitudes of 50 kHz) and under 50 kHz ^{1}H decoupling. Typically, ~20000 scans of 10 ms separated by a recycle delay of 3 s were collected.

NMR data analysis: The orientation of the backbone structures with respect to the membrane normal was characterized by two angles τ and ρ (SI Figure S2). The angle τ is the angle between the membrane normal n and the long axis of the molecule z, which was defined as the principal axis of the moment of inertia tensor corresponding to the smallest principal value. The angle ρ measures the rotation of the molecule around its long axis, and we define ρ=0° such that Cα of Pro^6 lies along (**n** x **z**) x **z**, where **n** is the membrane normal and **z** is the axis of the moment of inertia corrseponding to the long axis of the molecule. The splitting of the dipolar triplet in the ^{19}F-NMR-spectra, Δ_{FF}, or the signal position (chemical shift) in the ^{15}N-NMR spectra, δ_N, were analyzed as experimental data and compared with predicted (calculated) data to determine the best-fit backbone structure and membrane-alignment of harzianin HK-VI in lipid bilayers. Briefly, for a particular peptide orientation given by τ and ρ, the NMR-parameter (^{19}F-^{19}F dipolar coupling, or ^{15}N chemical shift) of the considered NMR label is predicted by converting the respective NMR-interaction tensor (^{19}F-^{19}F dipolar interaction tensor, or ^{15}N chemical shift anisotropy (CSA) tensor) from its principal axes frame representation to its laboratory frame representation. Averaging by molecular motions that are fast on the NMR-timescale was taken into account by scaling the anisotropic contribution to the resonance frequency with an order parameter S_{mol}, as indicated in Eq. 1 and Eq. 2. The deviation of the calculated NMR-parameters from the respective experimental values was quantified in terms of the root of mean square deviation (rmsd): rmsd = $(1/N\ \Sigma_k\ (d_{cal,k} - d_{exp,k})^2)^{1/2}$, with $d_{cal,k}$ and $d_{exp,k}$ denoting the calculated and experimental NMR-parameters (Δ_{FF} or δ_N), respectively, and N is the number of NMR-constraints. The principal axis values of the ^{19}F-^{19}F dipolar tensor and of the ^{15}N chemical shift anisotropy tensor were (-8 kHz, -8 kHz, 16 kHz) and (50 ppm, 74 ppm, 209 ppm), resulting into the maximum 19F dipolar splitting Δ_0 = 16 kHz, the ^{15}N isotropic chemical shift of δiso = 111 ppm, the ^{15}N chemical shift anisotropy δ_{CSA} = 98 ppm, and the ^{15}N asymmetry parameter of η = -0.245 (See Eq 1 and Eq. 2). The principal z-axis of the ^{15}N CSA tensor was assumed to be rotated 19° away from the N-H bond.

To identify the best-fit orientation and order parameter, the rmsd was determined for all combinations of τ and ρ within the range of [0°,180°] in steps of 1°, and for all S_{mol} within the range of [0,1] in steps of 0.1. (Note, that the values of τ and ρ were transformed to equivalent values of 180°-τ and 180° + ρ) This analysis was performed for all eight structure models, to find the best-fit secondary structure with the lowest overall rmds (SI Tables S6-S8).

Using the β-bend ribbon spiral conformation, we calculated the best-fit values of τ, ρ and S_{mol} for HZ for each of the five different patterns of labels (see SI Tables S9-S12). Each group gives a somewhat different solution, leading to an intrinsic scatter of values that contributes to the error margins. As the final values reported in Table 2, we took the average over the results of the individual analyses of the patterns of labels (SI Tables S9-S12).

Acknowledgements

The authors acknowledge Markus Schmitt (KIT, Karlsruhe) and Peter Gor'kov (NHMFL, Tallahassee) for building the probes used in this study and support of the NMR facility. We thankfully acknowledge financial support from the DFG-ANR grant "Peptaibols" (DFG: UL 127/6-1; ANR-2011-INTB-1002-01), the DFG grant INSTR 121384/58-1 FFUG, the Helmholtz Association program "BIF-TM" and in part the DFG-GRK (Nr2039).

Conflict of interest

The authors declare no conflict of interest.

Keywords: amino acids • peptides • membranes • isotopic labeling • NMR spectroscopy • fluorine

[1] I. Segalas, Y. Prigent, D. Davoust, B. Bodo, S. Rebuffat, *Biopolymers* **1999,** *50*, 71-85.
[2] R. Mikkola, M. A. Andersson, L. Kredics, P. A. Grigoriev, N. Sundell, M. S. Salkinoja-Salonen, *FEBS J.* **2012,** *279*, 4172-4190.
[3] L. Beven, D. Duval, S. Rebuffat, F. G. Riddell, B. Bodo, H. Wroblewski, *Biochim. Biophys. Acta Biomembr.* **1998,** *1372*, 78-90.
[4] I. Augeven-Bour, S. Rebuffat, C. Auvin, C. Goulard, Y. Prigent, B. Bodo, *J. Chem. Soc., Perkin Trans. 1* **1997,** 1587-1594.
[5] M. Lucaciu, S. Rebuffat, C. Goulard, H. Duclohier, G. Molle, B. Bodo, *Biochim. Biophys. Acta Biomembr.* **1997,** *1323*, 85-96.
[6] S. Rebuffat, H. Duclohier, C. Auvinguette, G. Molle, G. Spach, B. Bodo, *FEMS Microbiol. Immunol.* **1992**, *105*, 151-160.
[7] K. Koch, S. Afonin, M. Ieronimo, M. Berditsch, A. S. Ulrich, *Top. Curr. Chem*. **2012**, *306*, 89-118.
[8] D. Maisch, P. Wadhwani, S. Afonin, C. Böttcher, B. Koksch, A. S. Ulrich, *J. Am. Chem. Soc.* **2009**, *131*, 15596-15597.
[9] P. Wadhwani, E. Strandberg, J. van den Berg, C. Mink, J. Bürck, R. A. M. Ciriello, A. S. Ulrich, *Biochim. Biophys. Acta Biomembr.* **2014**, *1838*, 940-949.
[10] O. M. Michurin, S. Afonin, M. Berditsch, C. G. Daniliuc, A. S. Ulrich, I. V. Komarov, D. S. Radchenko, *Angew. Chem. Int. Ed.* **2016**, *55*, 14595-14599.
[11] F. Huguenot, T. Brigaud, *J. Org. Chem.* **2006**, *71*, 7075–7078.

[12] P. K. Mikhailiuk, S. Afonin, A. N. Chernega, E. B. Rusanov, M. O. Platonov, G. G. Dubinina, M. Berditsch, A. S. Ulrich, I. V. Komarov, *Angew. Chem. Int. Ed*. **2006**, *45*, 5659-5661.

[13] S. Afonin, U. H. N.; Dürr, P. Wadhwani, P., J. Salgado, A. S. Ulrich, *Top. Curr. Chem.* **2008**, *273*, 139-154.

[14] G. Chaume, N. Lensen, C. Caupene, T. Brigaud, *Eur. J. Org. Chem.* **2009**, *33*, 5717–5724.

[15] E. Devillers, J. Pytkowicz, E. Chelain, T. Brigaud, *Amino Acids* **2016**, *48*, 1457-1468.

[16] S. Rebuffat, S. Hlimi, Y. Prigent, C. Goulard, B. Bodo, *J. Chem. Soc., Perkin Trans.* **1996**, *1*, 2021-2027.

[17] L. Whitmore, B. A. Wallace, *Biopolymers* **2008**, *89*, 392-400.

[18] C. Toniolo, F. Formaggio, R. W. Woody in *Comprehensive Chiroptical Spectroscopy* (Eds.: N. Berova, P. L. Polavarapu, K. Nakanishi, R. W. Woody), John Wiley & Sons, Hoboken, **2012**, pp. 499–544.

[19] G. Yoder, T. A. Keiderling, F. Formaggio, M. Crisma, C. Toniolo, *Biopolymers* **1995**, *35*, 103–111.

[20] pdb codes: 5MF8 (structure in TFE); 5MF3 (structure in SDS); 5M9Y (structure in DPC); (to be published elsewhere).

[21] M. Putzu, S. Kara, S. Afonin, S. L. Grage, A. Bordessa, G. Chaume, T. Brigaud, A. S. Ulrich, T. Kubar, *Biophys. J.* **2017**, *112*, 2602-2614.

[22] R. Gessmann, H. Brückner, K. Petratos, *J. Pept. Sci.* ***2016****, 22, 76-81.*

[23] S. L. Grage, S. Afonin, A. S. Ulrich, *Methods Mol. Biol*. **2010**, *618*, 183-207.

[24] A. Grau-Campistany, E. Strandberg, P. Wadhwani, J. Reichert, J. Bürck, F. Rabanal, A. S. Ulrich, *Sci. Rep*. **2015**, *5*, 9388.

[25] E. Strandberg, D. Tiltak, S. Ehni, P. Wadhwani, A. S. Ulrich, *Biochim. Biophys. Acta Biomembr.* **2012**, *1818*, 1764-1776.

[26] E. Strandberg, J. Zerweck, P. Wadhwani, A. S. Ulrich, *Biophys. J.* **2013**, *104*, L9-L11.

[27] D. Windisch, C. Ziegler, S. L. Grage, J. Bürck, M. Zeitler, P. L. Gor'kov, A. S. Ulrich, *Biophys. J.* **2015**, *109*, 737-749.

[28] C. Muhle-Goll, S. Hoffmann, S. Afonin, S. L. Grage, A. A. Polyansky, D. Windisch, M. Zeitler, J. Bürck, A. S. Ulrich, *J. Biol. Chem.* **2012**, *287*, 26178-26186.

[29] R. W. Glaser, C. Sachse, U. H.N. Dürr, P. Wadhwani, A. S. Ulrich J. Magn. Reson. **2004**, *168*, 153–163

[30] D. S. Radchenko, S. Kattge, S. Kara, A. S. Ulrich, S. Afonin, *Biochim. Biophys. Acta Biomembr.* **2016**, *1858*, 2019-2027.

[31] Y. Shai, *Biopolymers* **2002**, *66*, 236-248.

[32] S. Zhang, X. Wu, M. Mehring, *Chem. Phys. Lett.* **1990**, *173*, 481-484.

10.1002/chem.201704307

WILEY-VCH

Entry for the Table of Contents (Please choose one layout)

FULL PAPER

A set of four orthogonal ^{19}F- and ^{15}N labels was developed for the structure determination of membrane bound peptides using solid-state NMR. Using this novel approach, which maximizes the information content employing only few labels, the secondary structure and orientation of a membrane-active peptaibol bound to lipid bilayers could be elucidated despite its short length and high mobility.

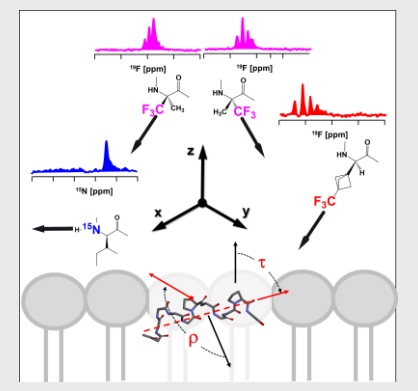

Stephan L. Grage, Sezgin Kara, Andrea Bordessa, Véronique Doan, Fabio Rizzolo, Marina Putzu, Tomáš Kubař, Anna Maria Papin[], Grégory Chaume, Thierry Brigaud, Sergii Afonin*, Anne S. Ulrich**

Page No. – Page No.

Orthogonal ^{19}F-labeling for solid-state NMR reveals the conformation and orientation of short peptaibols in membranes